

University of Groningen

A cellular and molecular model of response kinetics and adaptation in primate cones and horizontal cells

van Hateren, Hans

Published in:
 JOURNAL OF VISION

DOI:
[10.1167/5.4.5](https://doi.org/10.1167/5.4.5)

IMPORTANT NOTE: You are advised to consult the publisher's version (publisher's PDF) if you wish to cite from it. Please check the document version below.

Document Version
 Publisher's PDF, also known as Version of record

Publication date:
 2005

[Link to publication in University of Groningen/UMCG research database](#)

Citation for published version (APA):

van Hateren, H. (2005). A cellular and molecular model of response kinetics and adaptation in primate cones and horizontal cells. *JOURNAL OF VISION*, 5(4), 331-347. <https://doi.org/10.1167/5.4.5>

Copyright

Other than for strictly personal use, it is not permitted to download or to forward/distribute the text or part of it without the consent of the author(s) and/or copyright holder(s), unless the work is under an open content license (like Creative Commons).

The publication may also be distributed here under the terms of Article 25fa of the Dutch Copyright Act, indicated by the "Taverne" license. More information can be found on the University of Groningen website: <https://www.rug.nl/library/open-access/self-archiving-pure/taverne-amendment>.

Take-down policy

If you believe that this document breaches copyright please contact us providing details, and we will remove access to the work immediately and investigate your claim.

Downloaded from the University of Groningen/UMCG research database (Pure): <http://www.rug.nl/research/portal>. For technical reasons the number of authors shown on this cover page is limited to 10 maximum.

Small-signal analysis and Weber's law

Supplementary material to J.H. van Hateren (2005) A cellular and molecular model of response kinetics and adaptation in primate cones and horizontal cells. J.Vision

Basic model equations

A low-pass filter with time constant τ_y , transforming an input signal $x(t)$ into an output signal $y(t)$, is described by

$$\tau_y \dot{y} = x - y, \quad (1)$$

with the dot denoting time differentiation. Eq. (1) can be solved in the frequency domain. If $\tilde{y}(\omega)$ denotes the Fourier transform of $y(t)$, the Fourier transform of \dot{y} is given by $i\omega\tilde{y}$.

Fourier transforming both sides of Eq. (1) then gives

$$\tau_y i\omega\tilde{y} = \tilde{x} - \tilde{y}, \quad (2)$$

which yields the transfer function of the filter:

$$H(\omega) = \frac{\tilde{y}}{\tilde{x}} = \frac{1}{1 + i\omega\tau_y}. \quad (3)$$

Note that the low-frequency gain ($H(\omega)$ at $\omega \approx 0$) equals 1, thus low frequencies are not changed by the filter.

In the cone/horizontal cell model (see article), light I activates the visual pigment according to first-order kinetics, represented by a low-pass filter τ_R . Activated pigment produces activated G-protein, and finally activated PDE, E^* , again with first-order kinetics (τ_E). PDE reduces the concentration of cGMP at a rate

$$\beta = c_\beta + k_\beta E^*, \quad (4)$$

with c_β and k_β constants. The concentration X of cGMP, produced at a rate α , is then given by

$$\dot{X} = \alpha - \beta X, \quad (5)$$

or, equivalently,

$$\tau_X \dot{X} = \alpha \frac{1}{\beta} - X \quad \text{with } \tau_X = 1/\beta. \quad (6)$$

Opening of membrane channels by X gives a photocurrent

$$I_{os} = X^{n_x}, \quad (7)$$

partly consisting of calcium ions. Due to removal of calcium by an exchanger, the calcium concentration C is a low-pass filtered version of the photocurrent

$$\tau_c \dot{C} = I_{os} - C, \quad (8)$$

influencing the production of cGMP as

$$\alpha = \frac{1}{1 + (a_c C)^{n_c}}. \quad (9)$$

For the inner segment a membrane time constant τ_m is assumed, and its active membrane properties are modeled by assuming that the instantaneous conductance g_i approaches the steady-state conductance g_{is} according to first-order kinetics:

$$\tau_{is} \dot{g}_i = g_{is}(V_{is}) - g_i, \quad (10)$$

with

$$g_{is}(V_{is}) = a_{is} V_{is}^\gamma. \quad (11)$$

The signal subsequently enters the cone - horizontal cell feedback loop, where the signal in the horizontal cell is linearly subtracted from the cone signal before it drives the horizontal cell. For details about this part of the model see the article.

Small-signal analysis of the outer segment

Up to the point where activated PDE is produced, the system is assumed to be essentially linear, thus β is linearly related to the intensity I . I will below first analyze how the output of the outer segment, the photocurrent I_{os} , depends on changes in β if there would be no calcium feedback loop. This will give us a reference case with which we can compare the case when the calcium feedback loop is included.

Assuming that the calcium feedback loop is not functioning implies that the production rate of cGMP, α , is not modulated. It will be taken as a constant α_0 below. The remaining equations are then Eqs. (5) and (7), which we will now expand using

$$\begin{aligned}\beta &= \beta_0 + \Delta\beta \\ X &= X_0 + x \\ I_{os} &= I_{os,0} + i_{os}\end{aligned}\tag{12}$$

Here, as below, the small case symbols or the symbols with Δ represent small perturbations around a constant, steady-state value denoted by the subscript zero. Equation (5) then yields

$$\begin{aligned}\dot{X} = \dot{x} &= \alpha_0 - (\beta_0 + \Delta\beta)(X_0 + x) \\ &= \alpha_0 - \beta_0 X_0 - \beta_0 x - \Delta\beta X_0 - \Delta\beta x \approx -\beta_0 x - \Delta\beta X_0\end{aligned}\tag{13}$$

where the steady state of Eq. (5) was used ($\dot{X} = 0$ implies $\alpha_0 - \beta_0 X_0 = 0$), and $\Delta\beta x$ was neglected, because it is the product of two small numbers. Eq. (7) yields

$$\begin{aligned}I_{os,0} + i_{os} &= (X_0 + x)^{n_x} = X_0^{n_x} (1 + x/X_0)^{n_x} \approx X_0^{n_x} (1 + n_x x/X_0) \\ &= X_0^{n_x} + n_x X_0^{n_x-1} x\end{aligned}\tag{14}$$

which gives, because Eq. (7) implies $I_{os,0} = X_0^{n_x}$,

$$i_{os} = n_x X_0^{n_x-1} x.\tag{15}$$

Subsequently, Eqs. (13) and (15) are transformed to the frequency domain, where variables are denoted by a tilde. Because differentiating in the time domain corresponds to multiplying by $i\omega$ in the frequency domain, this yields

$$i\omega \tilde{x} = -\beta_0 \tilde{x} - \Delta\beta X_0,\tag{16}$$

and

$$\tilde{i}_{os} = n_x X_0^{n_x-1} \tilde{x}.\tag{17}$$

Therefore

$$\frac{\tilde{i}_{os}}{\Delta\beta} = \frac{-X_0 n_x X_0^{n_x-1}}{\beta_0 + i\omega} = \frac{-n_x X_0^{n_x}}{\beta_0 + i\omega} = \frac{-\tau_{\beta,0} n_x I_{os,0}}{1 + i\omega \tau_{\beta,0}}, \text{ with } \tau_{\beta,0} = 1/\beta_0.\tag{18}$$

This can be recognized as a low-pass filter with time constant $\tau_{\beta,0}$ and gain $-\tau_{\beta,0} n_x I_{os,0}$. The time constant is the time constant τ_X for $X = X_0$.

Including the calcium feedback loop strongly changes the behaviour of the circuit. In addition to Eqs. (12) we have

$$\begin{aligned}\alpha &= \alpha_0 + \Delta\alpha \\ C &= C_0 + c\end{aligned}\tag{19}$$

Eq. (13) then becomes

$$\dot{x} \approx \Delta\alpha - \beta_0 x - \Delta\beta X_0\tag{20}$$

or

$$\tilde{x} \approx \frac{\tilde{\Delta\alpha} - \tilde{\Delta\beta} X_0}{\beta_0 + i\omega}, \quad (21)$$

and we find an expression for $\Delta\alpha$ from Eq. (9):

$$\begin{aligned} \alpha_0 + \Delta\alpha &= \frac{1}{1 + a_c^{n_c} (C_0 + c)^{n_c}} = \frac{1}{1 + a_c^{n_c} C_0^{n_c} (1 + c/C_0)^{n_c}} \\ &\approx \frac{1}{1 + (a_c C_0)^{n_c} (1 + n_c c/C_0)} = \frac{1}{1 + (a_c C_0)^{n_c} + a_c^{n_c} n_c c C_0^{n_c-1}} \\ &= \frac{1}{(1 + (a_c C_0)^{n_c}) (1 + \frac{a_c^{n_c} n_c c C_0^{n_c-1}}{1 + (a_c C_0)^{n_c}})} \approx \frac{(1 - \frac{a_c^{n_c} n_c c C_0^{n_c-1}}{1 + (a_c C_0)^{n_c}})}{(1 + (a_c C_0)^{n_c})} \\ &= \alpha_0 - \alpha_0 \frac{a_c^{n_c} n_c c C_0^{n_c-1}}{1 + (a_c C_0)^{n_c}} = \alpha_0 - \beta_0 X_0 \frac{a_c^{n_c} n_c c C_0^{n_c-1}}{1 + (a_c C_0)^{n_c}} \end{aligned} \quad (22)$$

thus

$$\tilde{\Delta\alpha} = -\beta_0 X_0 \frac{n_c}{C_0} c_1 \tilde{c} \quad \text{with } c_1 = \frac{(a_c C_0)^{n_c}}{1 + (a_c C_0)^{n_c}}, \quad (23)$$

where the constant c_1 was defined for convenience of notation. Finally, Eq. (8) gives

$$\tau_c \dot{c} = I_{os,0} + i_{os} - C_0 - c = i_{os} - c \quad (24)$$

thus

$$\tilde{c} = \frac{\tilde{i}_{os}}{1 + i\omega\tau_c}. \quad (25)$$

From Eqs. (17), (21), (23), (25), $X_0^{n_x} = C_0$, and $X_0^{n_x} = I_{os,0}$ we obtain

$$\begin{aligned} \tilde{i}_{os} &= n_x X_0^{n_x-1} \tilde{x} = n_x X_0^{n_x-1} \frac{\tilde{\Delta\alpha} - \tilde{\Delta\beta} X_0}{\beta_0 + i\omega} \\ &= \frac{1}{\beta_0 + i\omega} (-n_x X_0^{n_x-1} \beta_0 X_0 \frac{n_c}{C_0} c_1 \tilde{c} - \tilde{\Delta\beta} n_x X_0^{n_x}) \\ &= \frac{1}{\beta_0 + i\omega} (-n_x n_c \beta_0 \frac{X_0^{n_x}}{C_0} c_1 \tilde{c} - \tilde{\Delta\beta} n_x X_0^{n_x}) \\ &= \frac{1}{\beta_0 + i\omega} (-n_x n_c \beta_0 c_1 \frac{\tilde{i}_{os}}{1 + i\omega\tau_c} - \tilde{\Delta\beta} n_x I_{os,0}) \end{aligned} \quad (26)$$

which finally yields the transfer function

$$H_{\beta,os} = \frac{\tilde{i}_{os}}{\tilde{\Delta\beta}} = \frac{-n_x I_{os,0}}{\beta_0 + \beta_0 n_x n_c c_1 / (1 + i\omega\tau_c) + i\omega}. \quad (27)$$

In the next two paragraphs, two major consequences of the processing in the outer segment will be discussed: the outer segment contributes to contrast constancy, and it regulates the bandwidth of the passed signal.

The calcium feedback loop corrects overshooting Weber's law

Without the calcium control loop, i.e. with fixed $\alpha = \alpha_0$, the photocurrent generated by small modulations in β at low frequencies ($\omega \approx 0$) follows from Eq. (18), using

$$I_{os,0} = X_0^{n_x} = (\alpha_0 / \beta_0)^{n_x}$$

$$\tilde{i}_{os} = -n_X \alpha_0^{n_X} \frac{\tilde{\Delta\beta}}{\beta_0^{n_X+1}} \sim \frac{\tilde{e}^*}{(c_\beta + k_\beta E_0^*)^{n_X+1}}. \quad (28)$$

where the latter follows from Eq. (4) and writing $E^* = E_0^* + e^*$. The \sim sign should be read as "is proportional to". For not too low background illuminances we have $k_\beta E_0^* \gg c_\beta$, which leads to

$$\tilde{i}_{os} \sim \frac{\tilde{i}}{I_0^{n_X+1}}, \quad (29)$$

where we have used the fact that E^* is proportional to the illuminance $I = I_0 + i$, i.e., E_0^* is proportional to I_0 , and e^* to i . For a value of $n_X = 1$, this shows that the current response \tilde{i}_{os} to an illuminance modulation \tilde{i} declines as $1/I_0^2$ with the background illuminance, and not as $1/I_0$ as required by contrast constancy. In other words, without calcium feedback the cone strongly overshoots Weber's law.

With a functioning calcium control loop, the photocurrent generated by small modulations in β at low frequencies ($\omega \approx 0$) follows from Eq. (27):

$$\tilde{i}_{os} = \frac{-n_X I_{os,0}}{\beta_0(1 + n_X n_C c_1)} \tilde{\Delta\beta}. \quad (30)$$

In this equation both $I_{os,0}$ and c_1 depend in a complicated way on β_0 , with $I_{os,0}$ the solution of

$$I_{os,0}^{1/n_X} + a_C^{n_C} I_{os,0}^{n_C/n_X} = 1/\beta_0, \quad (31)$$

and c_1 then given by

$$c_1 = \frac{(a_C I_{os,0})^{n_C}}{1 + (a_C I_{os,0})^{n_C}}. \quad (32)$$

In general, the dependence of $I_{os,0}$ on β_0 as shown in Eq. (31) can only be analyzed numerically. However, some insight into the behaviour of Eq. (30) can be obtained for the special case that $(a_C C_0)^{n_C} \gg 1$, corresponding to low to medium background illuminances. Then we find from Eq. (23) that $c_1 \approx 1$, and for $I_{os,0}$

$$I_{os,0} = X_0^{n_X} = \frac{\alpha_0^{n_X}}{\beta_0^{n_X}} = \frac{(1/(a_C C_0)^{n_C})^{n_X}}{\beta_0^{n_X}} = \frac{(1/(a_C I_{os,0})^{n_C})^{n_X}}{\beta_0^{n_X}}, \quad (33)$$

and therefore

$$I_{os,0} \sim \frac{1}{\beta_0^{n_X/(n_X n_C + 1)}} = \frac{1}{\beta_0^{0.2}}, \quad (34)$$

where the latter follows from assuming $n_X = 1$ and $n_C = 4$. Clearly, the steady-state current depends only weakly on β_0 . Then Eq. (30) finally results in

$$\tilde{i}_{os} \sim \frac{\tilde{i}}{I_0^{1.2}}, \quad (35)$$

using the same type of arguments that led to Eq. (29). This shows that the calcium feedback loop almost solves the problem of overshooting Weber's law. In the section "From linearity to contrast constancy" below I will show that the inner segment further alleviates the problem, and that it vanishes altogether when there is a suitable balance between c_β and k_β , the coefficients determining the dark and light activity of PDE.

The calcium feedback loop increases the frequency bandwidth

From Eq. (18) it is clear that without the calcium feedback loop, the small-signal transfer function from β to $I_{os,0}$ is a low-pass filter, with time constant depending on β_0 :

$$\frac{\tilde{i}_{os}}{\Delta\beta} = \frac{-\tau_{\beta,0}n_X I_{os,0}}{1+i\omega\tau_{\beta,0}}, \text{ with } \tau_{\beta,0} = 1/\beta_0. \quad (36)$$

With calcium feedback, the transfer function was derived in Eq. (27):

$$H_{\beta,os} = \frac{\tilde{i}_{os}}{\Delta\beta} = \frac{-n_X I_{os,0}}{\beta_0 + \beta_0 n_X n_C c_1 / (1+i\omega\tau_C) + i\omega}. \quad (37)$$

For large frequencies, with $\omega \gg 1/\tau_C$, the second term with β_0 in the denominator can be neglected, and the transfer function becomes identical to the case without calcium feedback. For $\tau_C = 3$ ms this implies a frequency considerably larger than 50 Hz. For low frequencies, with $\omega \ll 1/\tau_C$, $i\omega\tau_C$ can be neglected compared to 1, and the transfer function becomes

$$\frac{\tilde{i}_{os}}{\Delta\beta} = \frac{-\tau_{\beta}n_X I_{os,0}}{1+i\omega\tau_{\beta}}, \text{ with } \tau_{\beta} = 1/[\beta_0(1+n_X n_C c_1)], \quad (38)$$

which is a low-pass filter with a time constant and gain $(1+n_X n_C c_1)$ times smaller than the one of Eq. (36). The calcium feedback therefore in effect increases the response speed and frequency bandwidth of the photocurrent.

The general behaviour of Eq. (37) can be studied by rewriting it as

$$\frac{\tilde{i}_{os}}{\Delta\beta} = \frac{-n_X I_{os,0}(1+i\omega\tau_C)/\tau_C}{\omega_0^2 - \omega^2 + i\omega\gamma_0} \text{ with } \omega_0^2 = \frac{1+n_X n_C c_1}{\tau_C \tau_{\beta,0}} \text{ and } \gamma_0 = \frac{\tau_C + \tau_{\beta,0}}{\tau_C \tau_{\beta,0}}, \quad (39)$$

where the numerator has high-pass characteristics only relevant for high frequencies ($\omega > 1/\tau_C$), and the denominator can be recognized as a resonator with resonance frequency ω_0 and damping constant γ_0 . The quality factor Q of this resonator is then

$$Q = \frac{\omega_0}{\gamma_0} = \sqrt{1+n_X n_C c_1} \left(\frac{\sqrt{\tau_C \tau_{\beta,0}}}{\tau_C + \tau_{\beta,0}} \right). \quad (40)$$

The Q factor of a resonator quantifies the strength of resonance, where $Q < 0.5$ signifies an overdamped resonator, which shows no overshoots in response to a step and attains its steady-state slowly; $Q > 0.5$ signifies an underdamped resonator, which shows overshoots or even ringing in response to a step, and a clear resonance peak in the frequency transfer function; and $Q = 0.5$ signifies a critically damped resonator, which attains its steady-state in the fastest possible way without producing overshoots. Because $c_1 \leq 1$ (Eq. 32), the first factor in Eq. (40) is not larger than $\sqrt{5}$, assuming $n_X = 1$ and $n_C = 4$. The second factor is not larger than 0.5, for any value of τ_C and $\tau_{\beta,0}$, and therefore $Q \leq 0.5\sqrt{5} = 1.1$, indicating only mild underdamping at most. The actual value of Q depends, through c_1 , in an intricate way on the steady-state value of the photocurrent (Eq. 32). Figure 1 shows how the resonance frequency $\omega_0/2\pi$ and Q factor depend on background intensities between 1 and 1000 td, using the generic model parameters (defined in Table 1 of the article). The resonance frequency increases with background intensity, and the Q factor settles to values only slightly higher than the critically damped case.

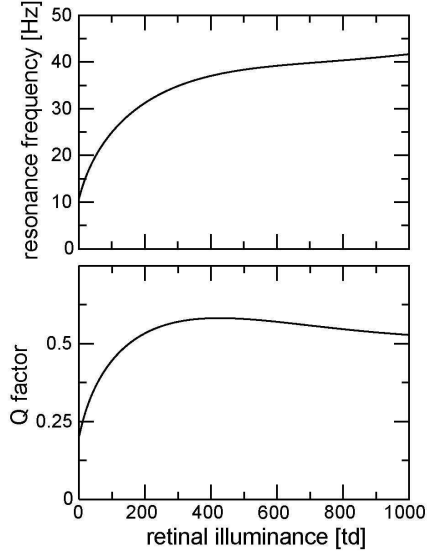


Figure 1. The resonance frequency and Q factor of the calcium control loop regulating the photocurrent generated in the cone outer segment.

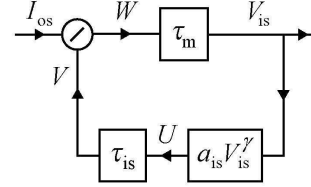


Figure 2. The control loop of the inner segment.

Small-signal analysis of the inner segment

The inner segment acts as a lead-lag element

The model of the inner segment is shown again in Figure 2, where a few additional variables are defined aiding the analysis. The equations describing this system are

$$\tau_m \dot{V}_{is} = W - V_{is}, \quad (41)$$

$$U = a_{is} V_{is}^\gamma, \quad (42)$$

$$\tau_{is} \dot{V} = U - V, \quad (43)$$

$$W = I_{os} / V. \quad (44)$$

Writing $I_{os} = I_{os,0} + i_{os}$, $W = W_0 + w$, $V_{is} = V_{is,0} + v_{is}$, $U = U_0 + u$, and $V = V_0 + v$, we can express the steady state value of $V_{is,0}$ in terms of that of $I_{os,0}$ as

$$V_{is,0} = (I_{os,0} / a_{is})^{1/(1+\gamma)}. \quad (45)$$

The small-signal expansion proceeds along similar lines as for the outer segment, and leads, after transforming to the frequency domain, to

$$i\omega\tau_m \tilde{v}_{is} = \tilde{w} - \tilde{v}_{is}, \quad (46)$$

$$\tilde{u} = a_{is} \gamma V_{is,0}^{\gamma-1} \tilde{v}_{is}, \quad (47)$$

$$i\omega\tau_{is} \tilde{v} = \tilde{u} - \tilde{v}, \quad (48)$$

$$\tilde{w} = \tilde{i}_{os} / V_0 - \frac{I_{os,0}}{V_0^2} \tilde{v}. \quad (49)$$

Eliminating \tilde{u} , \tilde{v} , and \tilde{w} from these equations gives the transfer function

$$\begin{aligned} H_{os,is} &= \frac{\tilde{v}_{is}}{\tilde{i}_{os}} = \frac{1}{V_0} \frac{1 + i\omega\tau_{is}}{(1 + i\omega\tau_{is})(1 + i\omega\tau_m) + \frac{I_{os,0}}{V_0^2} a_{is} \gamma V_{is,0}^{\gamma-1}} \\ &= \frac{V_{is,0}}{I_{is,0}} \frac{1 + i\omega\tau_{is}}{(1 + i\omega\tau_{is})(1 + i\omega\tau_m) + \gamma} \end{aligned} \quad (50)$$

where in the latter step $V_0 = a_{\text{is}} V_{\text{is},0}^\gamma$ and $V_0 = I_{\text{os},0} / V_{\text{is},0}$ were used. From the fits presented in the article we know that $\tau_{\text{is}} \gg \tau_{\text{m}}$, and we can therefore study the behaviour of this transfer function by approximating it as

$$\frac{\tilde{v}_{\text{is}}}{\tilde{i}_{\text{os}}} \approx \frac{V_{\text{is},0}}{I_{\text{is},0}} \frac{1 + i\omega\tau_{\text{is}}}{(1 + \gamma) + i\omega\tau_{\text{is}}}. \quad (51)$$

The second part of the right hand side of this equation acts as a lead-lag filter, with a low-frequency gain $1/(1 + \gamma)$ and a high-frequency gain of 1. With a value $\gamma = 0.7$ it thus acts as a mild high-pass filter, reducing low frequencies, and producing response sagging and rebounds in response to block-shaped stimuli.

Combining Eqs. (37) and (51) yields, to good approximation, for the combined transfer function of outer and inner segment

$$\frac{\tilde{v}_{\text{is}}}{\Delta\beta} = \frac{\tilde{v}_{\text{is}}}{\tilde{i}_{\text{os}}} \frac{\tilde{i}_{\text{os}}}{\Delta\beta} = \frac{-n_X V_{\text{is},0}}{[\beta_0 + \beta_0 n_X n_C c_1 / (1 + i\omega\tau_C)] + i\omega} \cdot \frac{1 + i\omega\tau_{\text{is}}}{(1 + \gamma) + i\omega\tau_{\text{is}}}. \quad (52)$$

From linearity to contrast constancy

Assuming $(a_C C_0)^{n_C} \gg 1$, we derived Eq. (34)

$$I_{\text{os},0} \sim \frac{1}{\beta_0^{n_X / (n_X n_C + 1)}}, \quad (53)$$

and Eq. (45) showed

$$V_{\text{is},0} \sim I_{\text{os},0}^{1/(1+\gamma)}. \quad (54)$$

Combining these two equations yields

$$V_{\text{is},0} \sim \frac{1}{\beta_0^{\left(\frac{n_X}{n_X n_C + 1}\right)\left(\frac{1}{1+\gamma}\right)}} = \frac{1}{\beta_0^{0.12}}, \quad (55)$$

where the latter follows from assuming $n_X = 1$, $n_C = 4$ and $\gamma = 0.7$. Thus the steady-state voltage depends even more weakly on β_0 than the steady-state current (Eq. 34).

Whether the system is linear or displays contrast constancy is in fact critically tuned by the activity of PDE. For low frequencies, using Eqs. (4), (52) and (55) we have

$$\tilde{v}_{\text{is}} \sim \frac{\tilde{e}^*}{(c_\beta + k_\beta E_0^*)^{1.12}}. \quad (56)$$

For the lowest background intensities $k_\beta E_0^* \ll c_\beta$, and this leads to

$$\tilde{v}_{\text{is}} \sim \tilde{e}^* \sim \tilde{i}, \quad (57)$$

showing that the cone voltage \tilde{v}_{is} responds linearly to a modulation \tilde{i} of the illuminance. For high background illuminances $k_\beta E_0^* \gg c_\beta$, which leads to

$$\tilde{v}_{\text{is}} \sim \frac{\tilde{e}^*}{E_0^{*1.12}} \sim \frac{\tilde{i}}{I_0^{1.12}}, \quad (58)$$

which is quite close to Weber's law, i.e., contrast constancy. Intermediate cases for the ratio of $k_\beta E_0^*$ and c_β may then be approximated by a dependence $\sim 1/I_0^\rho$, with ρ gradually shifting from 0 to 1.12 depending on light intensity. Thus the balance between c_β , the dark activity of PDE, and $k_\beta E_0^*$, the light-driven activity of PDE, is a major determinant of whether the system is linear ($\rho = 0$), is in a DeVries-Rose regime ($\rho = 0.5$), or displays full contrast

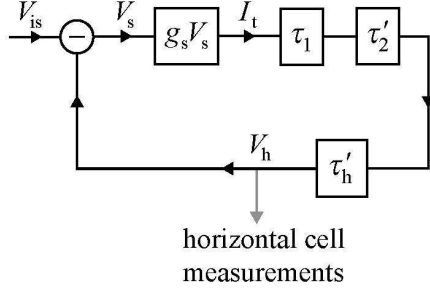


Figure 3. Linear version of the cone - horizontal cell feedback loop. V_{is} is the presynaptic membrane voltage in the cone, V_h the membrane voltage of the horizontal cell.

constancy ($\rho=1$). Obviously, this analysis is only approximate, because the assumption $(a_c C_0)^{n_c} \gg 1$ that led to Eq. (34) as implicitly used here is only valid for low to intermediate intensities.

The small-signal transfer function of cone and horizontal cell

Combining the appropriate equations above, we find for the overall transfer function of the cone

$$H_{\text{cone}} = \frac{-k_\beta n_X V_{is,0} (1 + i\omega\tau_{is})}{(1 + i\omega\tau_R)(1 + i\omega\tau_E)[\beta_0 + \beta_0 n_X n_C c_1 / (1 + i\omega\tau_C) + i\omega][(1 + i\omega\tau_{is})(1 + i\omega\tau_m) + \gamma]}, \quad (59)$$

with

$$\beta_0 = c_\beta + k_\beta I_0, \quad (60)$$

where I_0 is the background illuminance, and $V_{is,0}$ and c_1 are given by Eqs. (45) and (32), using $I_{os,0}$ as the solution of Eq. (31).

The small-signal transfer function of the cone - horizontal cell gain control loop (Figure 3) is analyzed as follows. For small signals, a_I (defined in the article) is constant to good approximation, and therefore also $\tau'_2 = a_I \tau_2$ and $\tau'_h = a_I \tau_h$ are constants. The gain g_s for small signals around a fixed value $V_{s,0}$ follows from the derivative of the function

$$I_t(V_s) = \frac{g_t / a_I}{1 + \exp(-(V_s - V_k)/V_n)}, \quad (61)$$

which yields a constant value for g_s :

$$g_s = \left. \frac{dI_t}{dV_s} \right|_{V_s=V_{s,0}} = \frac{g_t / (a_I V_n) \exp(-(V_{s,0} - V_k)/V_n)}{(1 + \exp(-(V_{s,0} - V_k)/V_n))^2}. \quad (62)$$

In the frequency domain one then finds for small signals

$$\tilde{v}_s = \tilde{v}_{is} - \tilde{v}_h, \quad (63)$$

$$\tilde{v}_h = g_s H_1 H_2 H_h \tilde{v}_s. \quad (64)$$

The transfer function of the low-pass filter τ_1 is $H_1 = 1/(1 + i\omega\tau_1)$, with similar transfer functions for τ'_2 and τ'_h . Eliminating \tilde{v}_s from these equations yields for the transfer function $H_{ch}(\omega)$ from cone to horizontal cell

$$H_{ch} = \frac{\tilde{v}_h}{\tilde{v}_{is}} = \frac{g_s H_1 H_2 H_h}{1 + g_s H_1 H_2 H_h} = \frac{g_s}{g_s + (H_1 H_2 H_h)^{-1}}. \quad (65)$$

The overall transfer function of the horizontal cell is then given by

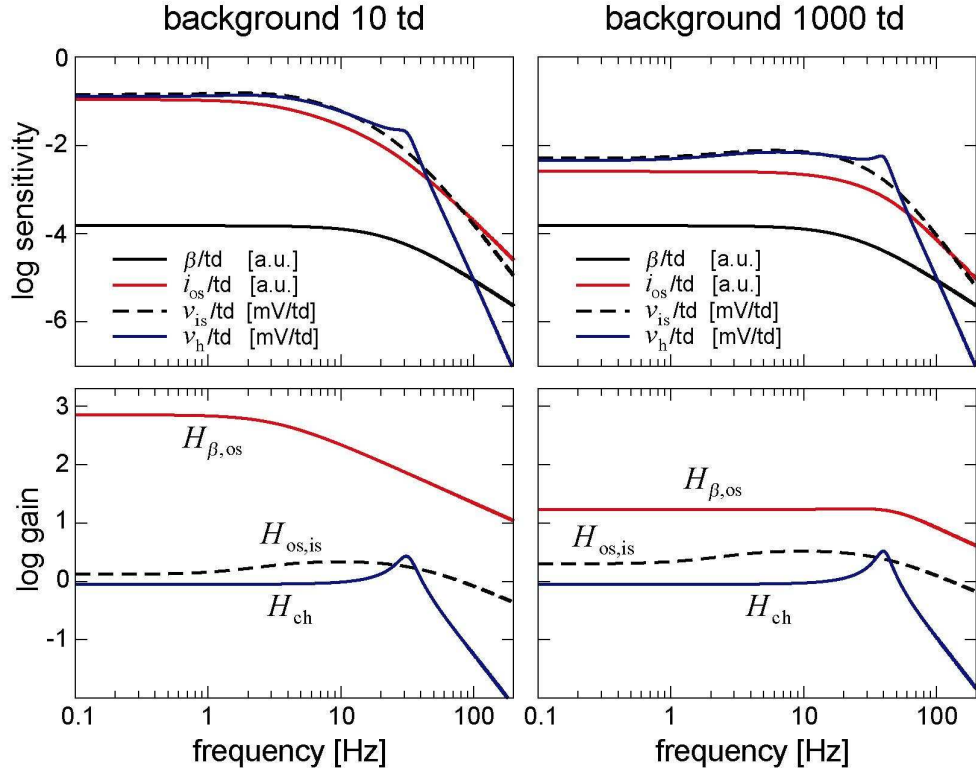


Figure 4. Sensitivity (response per unit illuminance modulation) as a function of frequency at various stages in the model (upper panels), and corresponding transfer functions (lower panels), at a background illuminance of 10 td (left column) and 1000 td (right column); β : PDE activity; i_{os} : photocurrent; v_{is} : membrane potential of cone; v_h : membrane potential of horizontal cell; $H_{\beta,os}$: transfer function from β to i_{os} ; $H_{os,is}$: transfer function from i_{os} to v_{is} ; H_{ch} : transfer function from v_{is} to v_h .

$$H_{hor.cell} = H_{cone} \frac{g_s}{g_s + (1 + i\omega\tau_1)(1 + i\omega\tau_2')(1 + i\omega\tau_h')} . \quad (66)$$

Figure 4 shows how the various components in the model contribute to building the transfer function of the cone and of the horizontal cell, where the parameters were used obtained from the fit to Figure 14A of the article. The left column was calculated for $I_0 = 10$ td, the right column for $I_0 = 1000$ td. The upper panels show the sensitivity, defined as the signal per unit illuminance modulation, of β , i_{os} (the photocurrent), v_{is} (the membrane potential of the cone inner segment) and v_h (the membrane potential of the horizontal cell). The amplitude of the corresponding transfer functions are shown in the lower panels, with $H_{\beta,os}$ the transfer function from β to i_{os} (Eq. 37), $H_{os,is}$ the transfer function from i_{os} to v_{is} (Eq. 50), and H_{ch} the transfer function from v_{is} to v_h (Eq. 65). Note that $H_{\beta,os}$ is the main factor responsible for the difference in transfer functions between 10 td and 1000 td, with a strong reduction in gain and increase in bandwidth at 1000 td compared with 10 td. The slight low-frequency fall-off in the sensitivity of v_{is} and v_h is due to $H_{os,is}$. Finally, the resonance observed at frequencies around 30-40 Hz is produced by H_{ch} . The latter is also responsible for the much steeper high-frequency fall-off of v_h compared with v_{is} .